The mouse HP1 proteins are essential for preventing liver tumorigenesis

Nehmé Saksouk, Shefqet Hajdari, Marine Pratlong, Célia Barrachina, Céline Graber, Damien Gregoire, Aliki Zavoriti, Amélie Sarrazin, Nelly Pirot, Jean-Yohan Noël, et al.

The mouse HP1 proteins are essential for preventing liver tumorigenesis

Nehmé Saksouk[1-4*], Shefqet Hajdari[1-4*], Yannick Perez[1-4], Marine Pratlong[5], Célia Barrachina[5], Céline Graber[6], Damien Grégoire[8-9], Aliki Zavoriti[1-4], Amélie Sarrazin[6], Nelly Pirot[1-4], Jean-Yohan Noël[1-4], Lakhdar Khellaf[4], Eric Fabbrizio[1-4, 8], Eric Julien[1-4, 8], Florence M. Cammas[1-4, 8]

[1] IRCM, Institut de Recherche en Cancérologie de Montpellier, Montpellier, F-34298, France.

[2] INSERM, U1194, Montpellier, F-34298, France.

[3] Université de Montpellier, Montpellier, F-34090, France.

[4] Institut régional du Cancer de Montpellier, Montpellier, F-34298, France.

[5] MGX, Biocampus Montpellier, CNRS, INSERM, Univ Montpellier, Montpellier, France

[6] IGBMC, Institut de Génétique, de Biologie Moléculaire et Cellulaire, Illkirch, France

[7] MRI, BioCampus Montpellier, CNRS, INSERM, Univ Montpellier, Montpellier, France

[8] CNRS, Route de Mende, Montpellier, France

[9] Institut de Génétique Moléculaire de Montpellier, University of Montpellier, CNRS, Montpellier, France

Corresponding author: Florence Cammas, Florence.cammas@inserm.fr

* Contributed equally to the work

Running title : HP1 prevent liver tumorigenesis

Abstract

Chromatin organization is essential for appropriate interpretation of the genetic information. Here, we demonstrated that the chromatin associated proteins HP1 are dispensable for hepatocytes survival but are essential within hepatocytes to prevent liver tumor development in mice with HP1β being pivotal in these functions. Yet, we found that the loss of HP1 *per se* is not sufficient to induce cell transformation but renders cells more resistant to specific stress such as the expression of oncogenes and thus *in fine*, more prone to cell transformation. Molecular characterization of HP1-Triple KO pre-malignant livers and BMEL cells revealed that HP1 are essential for the maintenance of heterochromatin organization and for the regulation of specific genes with most of them having well characterized functions in liver functions and homeostasis. We further showed that some specific retrotransposons get reactivated upon loss of HP1, correlating with over-expression of genes in their neighborhood. Interestingly, we found that, although HP1-dependent genes are characterized by enrichment H3K9me3, this mark does not require HP1 for its maintenance and is not sufficient to maintain gene repression in absence of HP1. Finally, we demonstrated that the loss of TRIM28 association with HP1 recapitulated several phenotypes induced by the loss of HP1 including the reactivation of some retrotransposons and the increased incidence of liver cancer development. Altogether, our findings indicate that HP1 proteins act as guardians of liver homeostasis to prevent tumor development by modulating multiple chromatin-associated events within both the heterochromatic and euchromatic compartments, partly through regulation of the corepressor TRIM28 activity.

Keywords: chromatin; HP1; cancer; liver; transcriptional silencing; endogenous retrovirus

Introduction

Chromatin organization is essential for the interpretation of genetic information in a cell-type and tissue-specific manner [1]. Alteration of this organization can have devastating consequences, as evidenced by the large number of diseases induced by mutations in chromatin-associated proteins [2,3], as well as by the dramatic changes in chromatin organization observed in cancer cells [4]. Although extensively studied in the past three decades, it is still poorly understood how chromatin organization is regulated and involved in tumorigenesis.

Chromatin can be divided according to its structural and functional features in euchromatin and heterochromatin. Euchromatin displays low level of compaction, is highly enriched in genes, and is transcriptionally competent. Conversely heterochromatin is highly compacted, enriched in repetitive DNA sequences, and mostly silent [5]. Heterochromatin Protein 1 (HP1) proteins, first isolated as major heterochromatin components in *Drosophila*, are highly conserved from yeast to mammals which express three isoforms (HP1α, HP1β and HP1γ) that are distributed in both eu- and heterochromatin [6]. These proteins are characterized by a chromodomain (CD) involved in recognition of H3 lysine-9 di- or trimethylated (H3K9me2/3), and a chromoshadow domain (CSD), which, through dimerization, constitutes a platform for interaction with many protein partners. These two domains are separated by the hinge domain involved in HP1 association with RNA and recruitment to heterochromatin [7,8]. Accordingly, HP1 are important for heterochromatin organization and silencing, chromosome segregation, gene expression, DNA repair, DNA replication and for genome stability [9–11],[12,13]. Several studies suggested a correlation between the level of HP1 expression and cancer development and/or metastasis. However, how HP1 are involved in these processes remains largely to be clarified [14,15].

Liver chromatin organization has been well characterized in several physio-pathological conditions [16]. In addition, several known HP1 partners, including the transcription cofactors TRIM24 and TRIM28, and the histone-lysine N-methyltransferase

SUV39H1 have been shown to play key roles in hepatocytes [17–21]. Together, this prompted us to further characterize HP1 functions in liver through inactivation of all HP1 encoding genes specifically in mouse hepatocytes. Here, we demonstrated that HP1 are dispensable for hepatocytes survival but essential to prevent tumor development. We further identified alterations of heterochromatin organization, of gene expression and of silencing of specific ERVs through deregulation of the corepressor TRIM28 activity, all these features being most likely key players in the process of tumorigenesis

RESULTS

HP1 proteins are dispensable for hepatocyte survival but essential to prevent liver tumor development

To investigate HP1 *in vivo* functions, the HP1β and HP1γ encoding-genes (*cbx1* and *cbx3,* respectively) were inactivated individually or together in the liver of either WT or HP1αKO mice [22] using the Cre recombinase expressed under the control of the hepatocyte-specific albumin promoter [23,24]. This led to different liver-specific combinations of HP1 knockout (KO) models as indicated in Figure 1A. Liver-specific excision of the *cbx1* and *cbx3* alleles was confirmed by PCR and the level of HP1 proteins was checked by western blotting and immunofluorescence (IF) as illustrated for animals having all HP1-encoding genes inactivated in hepatocytes (thereafter called HP1-TKO) (Fig. 1B and Fig. S1A-B). Note that because of the germ cell excision of *cbx5*, HP1α was not expressed in any cells of mice models carrying the $cbx5^{-/-}$ alleles (Fig. 1B).

HP1-mutant mice were morphologically similar to their control counterparts throughout their all life. However, autopsies of old animals revealed that all HP1-mutant animals developed liver tumors with a higher incidence than control animals and with the loss of HP1β having the strongest effect as compared to the loss of HP1α or HP1γ (Figure 1C-D). Analysis of the floxed *cbx*1 and *cbx*3 gene excision confirmed that tumors originated from HP1-mutant hepatocytes (Fig. S1E). Since the loss of the HP1 isoforms display additive effect on tumor incidence, we focus most of the following analysis on HP1-TKO livers.

Histological analysis of liver sections from young and middle-aged HP1-TKO animals did not reveal any significant alteration of the structural organization of hepatocytes nor of the liver parenchyma (Fig. S1C), whereas most old HP1-TKO animals developed tumor nodules that could easily be distinguished from the rest of the liver parenchyma (Fig. 1E). These nodules were characterized by the presence of well-differentiated hepatocytes but without

their specific trabecular organization, and thus, were identified as typical hepatocellular carcinoma (HCC). Analysis of proliferation (Ki67), apoptosis (Activated caspase 3) and the presence of DNA breaks (γH2AX[25]) by immuno-histochemistry (IHC) of Tissue Micro Arrays (TMA) containing liver sections did not reveal any significant difference of proliferation between young and middle-aged mutant and control animals (Fig. S1D) but a two-fold increase in both the tumoral (TKOT) and non-tumoral (TKON) parts of HP1-TKO livers compared with controls. No change was detected in the number of apoptotic- nor γH2AX-positive cells at any age.(Fig. S1D-E).

We then tested by RT-qPCR the expression of several genes frequently altered in human HCC [26]. *Arid1A*, *Trp53*, *E2f1* and *E2f7* were significantly over-expressed in HP1-TKO (Fig. 1F). Moreover, α-fetoprotein (*Afp*), a marker of human HCC [27], was strongly over-expressed exclusively in the tumor tissue of three of the five tested tumors (Fig. 1F). Altogether, these data demonstrated that HP1 proteins are dispensable within hepatocytes but they are additionally involved to prevent tumor development, with HP1β being pivotal in this function.

Loss of HP1 increases intrinsic transformation potential of BMEL cells

To unambiguously test the viability of hepatic cells in absence of any HP1 isoform, bipotential hepatic BMEL (Bipotential Mouse Embryonic Liver) cell lines were established according to the protocol described by Strick-Marchand & Weiss [28]. All HP1 encoding genes were inactivated in these cells as illustrated in Figure 2A. These cells, thereafter called HP1-TKO cells, were morphologically similar but had a tendency to proliferate faster than control cells (Fig. 2B). To determine whether the loss of HP1 intrinsically induced tumorigenic properties in BMEL cells, we first tested the ability of single cells to form colonies in presence or absence of HP1. As illustrated in Figure 2C, HP1-TKO cells formed more colonies than control cells. However, none of these cells were able to grow on soft agar (data not shown). Because oncogenic stress is a well-known factor of tumorigenesis and since that several genes with putative oncogenic activities were over-expressed in HP1-TKO livers (*BMyc*, *Ect2*, *Mas1*, *Mycl*, *Rab27a*, *Rabl2* and *Src*), we tested the response of control and HP1-TKO

cells to the expression of the oncogenes H-RasV12 and SV40 either alone or in combination. H-RasV12 alone or with SV40 lead to massive cell death as well as to senescence as measured by the expression of β-galactosidase, in control but not HP1-TKO cells (Fig. 2D and Fig. S2A-B). Conspicuously, both control and HP1-TKO BMEL cells expressing H-RasV12 and SV40 but not H-RasV12 alone were able to form colonies in soft agar however, HP1-TKO cells formed more colonies than control cells (Fig. 2E and data not shown). Altogether, these data indicated that the loss of HP1 *per se* did not lead to cell transformation but increased the potential of BMEL cells to get transformed upon expression of oncogenes.

Since we identified HP1β as essential for preventing liver tumor development (Fig.1C-D), we wondered whether its expression was sufficient to restore the phenotype induced by HP1 inactivation. We thus established BMEL HP1-TKO lines expressing HP1β in fusion with the fluorophore YFP and found that it was indeed sufficient to decrease the ability of HP1-TKO cells to form colonies in soft agar in response H-RasV12 and SV40 expression (Fig. 3B, lanes 6-7 and Fig. S2C).

Heterochromatin organization is altered in HP1-TKO hepatocytes

We next initiated molecular characterization of both HP1-TKO pre-malignant livers and HP1-TKO BMEL cells. As shown in Figure 3A, H3K9me3 and H4K20me3, two marks of constitutive heterochromatin, were strongly decreased in the liver of young and middle-aged HP1-TKO mice compared with age-matched controls. Conversely, no change of H3K27me3 nor of H3K9me2, H4K20me2 and H4K20me1 was observed in these same samples (Fig. 3A). The specific decrease of H3K9me3 and H4K20me3 was also observed in HP1-TKO BMEL cells (Fig. 3B lanes 1 to 5) and importantly, it was restored by expression of HP1β-YFP (Fig. 3B lanes 6-7). Further, IF analysis in BMEL cells, indicated that only H3K9me3 associated with chromocenters (i.e., DAPI-dense structures that contain structural components of heterochromatin) was drastically reduced in HP1-TKO cells, whereas the labeling within euchromatin was not significantly affected (Fig. 3C). The level and distribution of 5-methyl cytosine (5mC) were not altered in HP1-TKO BMEL cells (Fig. 3C). Although

HP1-TKO chromocenters clustered, quantification of the intensity of DAPI staining indicated that it was roughly homogeneously distributed throughout control nuclei, whereas it was increased progressively from the inner to the external part in HP1-TKO nuclei (Fig. 3D). Yet, this was not associated with any significant change in the level nor distribution of laminB1 (LamB1) (Fig. 3C).

Finally, we tested whether the decrease of pericentromeric H3K9me3 was associated with a decrease of this mark on Major Satellite repeats, the main component of pericentromeric heterochromatin. To this end, we performed H3K9me3 and H3K27me3 chromatin immunoprecipitation (ChIP) in BMEL cells and found that H3K9me3, but not H3K27me3, was completely lost on Major Satellites (Fig. 3E). Yet, we did not observe any over-expression of these repeats which even had a tendency to be down-regulated in absence of HP1 in both liver and BMEL cells (Fig. 3F). Similarly, there was no change in the number of these repeats within the liver genome (Fig. 3G). These data demonstrated that HP1, notably HP1β, are essential in hepatocytes for the maintenance of constitutive heterochromatin histone marks and for the sub-nuclear organization of chromocenters, but not for the expression or the stability of major satellites.

HP1 proteins are involved in the regulation of specific gene expression programs

To investigate the role of HP1 in the regulation of gene expression in liver, we performed an unbiased RNA-seq transcriptomic analysis of libraries prepared from 7 week-old control and HP1-TKO liver RNA. We found that 1215 genes were differentially expressed (730 up-regulated and 485 down-regulated) between control and HP1-TKO livers (with a 1.5-fold threshold difference and an adjusted $P \leq 0.05$) (Fig. 4A and supplementary Table 1). Analysis of differentially expressed genes (thereafter called HP1-dependent genes) using David Gene Ontology (https://david.ncifcrf.gov/) and Gene Set Enrichment Analysis (GSEA; http://software.broadinstitute.org/gsea/index.jsp) softwares revealed that several biological processes were significantly affected in HP1-TKO livers. First, there was a very high

enrichment of genes encoding for the Krüppel Associated Box (KRAB) domain within up-regulated genes (*P* = 5.8E-26) (Fig. 4B & Supplementary Tables 1; 2 & 3) which was-validated by RT-qPCR (Fig. 4C). Up-regulated genes were also enriched in genes belonging to the GO terms signal peptide, immunity, guanylate-binding protein and response to virus (Fig. 4B), suggesting activation of an inflammatory response in HP1-TKO livers (Fig. 4B-C & Supplementary Table 4). Genes encoding for members of the p450 cytochrome (CYP) family were also strongly enriched in HP1-dependent genes with 7 up-regulated and 18 down-regulated amongst the 79 CYP genes detected in the present RNAseq analysis. In particular, 11 *cyp2* family genes were involved in Endoplasmic Reticulum (ER) and redox functions that are known to be essential for liver homeostasis [29,30,31] (Table 1). Moreover, *Nox4* (nicotinamide adenine dinucleotide phosphate (NADPH) oxidase 4), a gene consistently associated with ER and ROS in liver [32], was significantly down-regulated in HP1-TKO as compared with control livers (Fig. 4C & Supplementary Table 1). In line with these results, oxidation-reduction, ER, steroid hormone biosynthesis, lipid metabolic process were amongst the most affected functions in HP1-TKO livers (Fig. 4B & Supplementary Tables 2; 3; 5 and 6). The differential expression of *Cyp2c29* and *Cyp2b10* (ER and redox), *Ifit2* (interferon γ signature) and *Nox4* (ROS production) was validated by RT-qPCR in 7 week-old HP1-TKO and control livers (Fig. 4C).

As mentioned above, the simultaneous loss of HP1α and HP1β also led to high incidence of liver tumor development (Fig. 1C-D). To identify genes commonly deregulated in HP1-TKO and HP1αβ-liverKO livers that might explain the tumor protective role of HP1, we performed a RNAseq analysis in HP1αβ-liverKO (GSE84734). Only 18 genes (13- up and 5 down-regulated) were similarly deregulated in HP1αβ-liverKO and HP1-TKO livers (supplementary table 7). Interestingly, on the 13 up-regulated genes, 5 belonged to the family of transcriptional repressors KRAB-Zinc Finger Proteins (KRAB-ZFP). We thus analyzed the expression of several of these *krabzfp* genes by RT-qPCR in HP1αβ-liverKO, HP1αγ-liverKO and control livers. As illustrated in Figure 4D, *zfp951* and *zfp992* were up-

regulated exclusively in HP1αβ-liverKO livers, *zfp345*, exclusively in HP1αγ-liverKO livers whereas *zfp984* and *5730507C01Rik* were up-regulated in both HP1αβ-liverKO and HP1αγ-liverKO livers. These results demonstrated specific and redundant functions for the different HP1 isoforms and that HP1β has specific functions for the regulation of *zfp951* and *zfp992* genes that could thus be determinant in the HP1-dependent tumorigenesis process.

HP1 loss lead to reactivation of specific retrotransposons and over-expression of neighboring genes

KRAB-ZFP are transcriptional repressors known to repress themselves and retrotransposons of the endogenous retroviruses (ERV) family [33,34]. To determine whether the HP1-dependent deregulation of KRAB-ZFP was associated with altered ERV expression in liver, we investigated the expression of DNA repeats in our RNA-seq dataset. Coordinates of all annotated DNA repeats of the RepeatMasker database (mm10 assembly) were aligned against the RNA-seq reads and only those that could be assigned unambiguously to a specific genomic locus were analyzed. In total, 846 repeats were deregulated in HP1-TKO compared with control livers with 71.3% being up-regulated and 28.7% down-regulated (Fig. 5A & Supplementary Table 8). Among up-regulated repeats, 59.4% were ERV, 19.2% long interspersed nuclear elements (LINEs) and 9.3% short interspersed elements (SINEs) supporting the hypothesis that HP1 were preferentially involved in ERV silencing in liver (Fig. 5B & Supplementary Table 8).

To assess the putative link between ERV and gene expression, we first mapped HP1-dependent repeats located within 100kb surrounding HP1-dependent genes. This analysis showed that a fraction of HP1-dependent genes (138 up-regulated and 94 down-regulated) was associated with HP1-dependent repeats. Interestingly, this physical association correlated with a functional association since 84% of repeats associated with up-regulated genes were also up-regulated and 75.5% of repeats associated with down-regulated genes were down-regulated (Fig. 5C & Supplementary Tables 9 & 10). Furthermore, up-regulated

repeats tended to be located closer to up-regulated genes than to down-regulated genes, and vice versa (Fig. 5D). Altogether, this analysis strongly suggested a link between loss of HP1, loss of KRAB-ZFP repressive activity, ERV reactivation and up-regulation of genes in their neighborhood. Accordingly, several deregulated genes associated with deregulated repeats such as *Mbd1*, *Bglap3*, *Obpa*, *Bmyc*, *Fbxw19* and *Zfp445* were already shown to be controlled by ERVs (Fig. 5E and [35,36]).

HP1 loss has gene-specific impact on H3K9me3 deposition

KRAB-ZFPs regulate their targets through recruitment of the corepressor TRIM28 and of the Histone Methyl Transferase (HMT) SETDB1 for the establishment of a heterochromatin-like environment characterized by H3K9me3 enrichment [37]. To first test whether the KRAB-ZFP/ERV pathway was also deregulated in HP1-TKO BMEL, we measured the expression of *Zfp345*; *Zfp951, zfp992, Bglap3* and *Cyp2b10* in control and HP1-TKO BMEL cells. As in HP1-TKO livers, all these genes were over-expressed in HP1-TKO versus control BMEL cells (Fig. 5F). Control level of expression was rescued by HP1β-YFP for *Zfp951, zfp992, Bglap3* and *Cyp2b10* but not for *Zfp345* in agreement with our observation that this latter gene was deregulated in HP1αγ-liverKO but not HP1αβ-liverKO livers (Fig. 4D and Fig. 5G). Several *krabzfp* genes were characterized by an enrichment of H3K9me3 preferentially at their 3'UTR [34]. We therefore tested the enrichment of this mark at the 3'UTR of *zfp345*, *zfp951* and *zfp992* as well as at three previously described positions of *Bglap3* gene associated with a IAP [35]. In control BMEL cells, H3K9me3 was highly enriched at the 3' UTR of all *krabzfp* genes, on the three positions associated with *Bglap3* as well as in the promoter region of *Cyp2b10* as compared to the housekeeping gene *36B4* (Fig. 5H). In HP1-TKO BMEL cells, H3K9me3 was significantly decreased at *zfp345* and *zfp992* genes. However, in striking contrast it was unchanged at *zfp951*, at the P2 and IAP positions of the *Bglap3* locus as well as at *Cyp2b10* and was even increased at the *Bglap3* p4 position (Fig. 5H). These results indicated that HP1-dependent loci are characterized by enrichment of

H3K9me3 which does not require HP1 for its maintenance and which is not sufficient to repress the expression of the associated genes in absence of HP1.

HP1 is necessary for TRIM28 activity within liver

To better characterize the relationship between HP1, KRAB-ZFPs, TRIM28 and ERVs, we first checked the expression of TRIM28 in HP1-TKO livers. This analysis showed that TRIM28 expression was not significantly altered in HP1-TKO (Fig. 6A-B). We then used the previously described mouse models in which either a mutated TRIM28 protein that cannot interact with HP1 (T28HP1box) replaces TRIM28 or in which TRIM28 is depleted (T28KO) specifically within liver [17,38]. As expected, TRIM28 expression was strongly decreased in T28KO livers, whereas it was only marginally decreased in T28HP1box livers (Fig. 6C). The level of all three HP1 was not affected in these mouse strains (Fig. 6C). RT-qPCR analysis showed that several HP1-dependent genes including *Nox4*; *Cypc29* and *Rsl1* were not affected in T28HP1box and T28KO livers (Fig. 6D). Conversely, *Cyp2b10; Ifit2*; *Zfp345* and *Zfp445* that were all over-expressed in HP1-TKO liver were also up-regulated in T28HP1box and T28KO livers (Fig. 6D). To test whether the HP1-dependent ERV-associated genes required TRIM28, the expression of *Mbd1* and *Bglap3* was assessed in T28KO and T28HP1box livers. Like in HP1-TKO livers, both genes were over-expressed in T28KO and T28HP1box livers, although to a lesser extent as compared to HP1-TKO livers (Fig. 6E). Finally, analysis in old animals (Fig. 6G-H) showed that both genes were over-expressed in the normal (TKON) and tumor (TKOT) liver parts from old HP1-TKO animals whereas *Mbd1* was no longer over-expressed in old TRIM28 mutant mice livers. *Bglap3*, was slightly over-expressed in T28KO but not in T28HP1box old animals (Fig. 6G-H).

As for HP1-TKO mice, old T28KO and T28HP1box mice developed more liver tumors than controls, although with a lower incidence than HP1-TKO animals (32.4% and 33.5% for T28KO and T28HP1box respectively, Fig. 6F). Altogether, these data suggested that HP1 prevented liver tumor development at least partially by sustaining TRIM28 repressive activity.

DISCUSSION

In this study, we demonstrated that HP1 proteins and in particular HP1β are essential within hepatocytes to prevent development of hepatocellular carcinoma (HCC) in mice. We further showed that HP1 are pivotal within hepatocytes for appropriate expression of liver specific genetic programs and for organization of pericentromeric heterochromatin. Last we present several lines of evidence that HP1 are acting as barrier against liver tumor development at least partially by keeping specific sets of retrotransposons silent through regulation of TRIM28 corepressor activity.

The finding that HP1 proteins were not essential for neither cell viability nor liver function was in contrast with many studies showing the fundamental functions of each HP1 isoform in various pluripotent and differentiated cellular systems [39,40] as well as during embryonic development in various species, such as *Drosophila* [41], C. *elegans* [42]. However, it is important to note that liver has very specific properties, being mostly quiescent throughout life but able to regenerate upon stress essentially through the re-entry of quiescent and fully differentiated hepatocytes into cell cycle rather than via stem cell proliferation, as it is the case in other tissues [43,44]. These specific properties of hepatocytes could rely on a peculiar loose chromatin organization that might be less sensitive to the loss of HP1 as compared to other cell types for cell viability but more prone to cell transformation as we observed in BMEL cells. In support of this hypothesis, it is noteworthy that, among the 17 human cancers tested in the database from Human Protein Atlas (https://www.proteinatlas.org and Fig. S3), liver cancer is the one expressing the lowest levels of *cbx1*, *3* and *5*. These data strongly suggest that in Human, as in mice, low level of HP1 expression is determinant for the initiation of liver tumorigenesis. Strikingly however, high levels of *cbx1*, *3* and *5* expression are all unfavorable prognostic markers in liver cancer (https://www.proteinatlas.org and Fig. S3), suggesting that the levels of HP1 have to be tightly regulated in liver and that HP1 could have different functions at different stages of cancer development as it has been proposed by Lee & Ann [45] for breast cancer. Interestingly, we showed here, that the increased cellular

sensitivity to transformation induced by the loss of HP1 is reversible and can be rescued by the sole re-expression of HP1β suggesting that regulating the level of HP1 could be a therapeutic strategy for liver cancer.

We further demonstrated that HP1 are essential within hepatocytes for the maintenance of H3K9me3 and H4K20me3 at pericentromeric heterochromatin and for appropriate localization of DAPI-dense structures. These results are in line with the demonstration that in worms, inactivation of the two H3K9 methyltransferases Met-2 (me1 and me2) and SET-25 (me3) is necessary to trigger heterochromatin release from the nuclear periphery whereas inactivation of either one or the other is insufficient [46]. However these results are in contrast with studies suggesting that HP1 is required to trigger attachment of heterochromatin to the nuclear periphery [47]. Furthermore, in contrast to the results reported upon loss of H3K9me3 induced by inactivation of the histone methyltransferases SUV39H1 and SUV39H2, the loss of H3K9me3 on major satellite repeats in HP1-TKO hepatocytes did not result in neither decrease of H3K9me2 nor in over-expression of these major satellite repeats [48,49]. This observation suggests that in liver, H3K9me2 maintenance is independent of HP1 and is sufficient to keep major satellite repeats at a low level of transcription even in absence of HP1. SUV39H1 over-expression has been reported to be associated with HCC development [18] and HCC induced by a methyl-free diet is also characterized by elevated SUV39H1 expression and increased H3K9me3 but with reduced H4K20me3 deposition [50]. This suggests that the global decreased level of H4K20me3 rather than of H3K9me3 in HP1-TKO mice could be a key determinant of tumorigenesis. In support of this hypothesis, H4K20me3 was reported to be essential for genome integrity and for proper timing of heterochromatin replication whose deregulation has recently been proposed to be involved in cancers [51–53]. Our results highlight complex interplay between heterochromatin components for the organization of this compartment that is likely essential to prevent tumor development. As reported by others, we found that HP1 are involved in both repression and activation of gene expression [7,54–56]. Interestingly,

351 although HP1-dependent genes are characterized by enrichment in H3K9me3, this mark
352 remains mostly unchanged upon HP1 inactivation but is not sufficient to maintain gene
353 repression. These results are reminiscent to those obtained in yeast showing that H3K9me3
354 can be maintained in absence of HP1 through association with a RNA-induced transcriptional
355 silencing complex[57].

356 Functionally, many HP1-dependent genes are involved in liver specific functions. In
357 particular, several belong to the p450 cytochrome family (Cyp) which is involved in liver
358 detoxification, in oxidative stress and homeostasis of the endoplasmic reticulum that are
359 three key factors in hepatocarcinogenesis [58]. How these genes are regulated by HP1
360 remains to be determined. However nuclear receptors of the Peroxisome Proliferation-
361 Activated Receptors (PPAR) were shown to be important in this process and PPARγ is
362 strongly down-regulated in HP1 mutant mice [59]. It is thus tempting to speculate that this low
363 expression of PPARγ underlies the deregulation of several *Cyp* genes. Furthermore, HP1-
364 TKO livers were also characterized by a transcriptional signature of an interferon γ response
365 strongly suggesting liver inflammation, a factor associated with 90% of hepatocarcinogenesis
366 [60 61 62]. Over-expression of retrotransposons *per se* was shown in some circumstances to
367 lead to inflammation through activation of the cGAS-STING pathway [63]. As we have
368 demonstrated that the loss of HP1 reactivates specific retrotransposons, we can hypothesize
369 that they cause inflammation and thus a favorable environment for HCC development.

370 Finally, we demonstrated that the loss of HP1 lead to partial loss of TRIM28 activity
371 characterized by reactivation of a specific set of retrotransposons associated with over-
372 expression of genes in their neighborhood. Moreover, we showed that the loss of interaction
373 between TRIM28 and HP1 within hepatocytes is sufficient to partially recapitulate the
374 phenotypes induced by HP1 or TRIM28 inactivation. Consistent with our results, SETDB1,
375 the main H3H9 methyltransferase associated with TRIM28 and KRAB-ZFP for ERV silencing
376 [64,65] was identified as a human hepatic cancer driver gene (IntOgen,
377 http://www.intogen.org/mutations/). Together, these results strongly suggest that

deregulation of the KRAB-ZFP/TRIM28/SETDB1 pathway is determinant in HP1-dependent tumorigenesis[33,66,67].

In conclusion, we identified HP1 proteins as key players to prevent liver tumorigenesis. We further present evidence that this function of HP1 as guardian of liver homeostasis relies on regulation of heterochromatin organization, gene expression and ERV silencing.

MATERIALS AND METHODS

Mouse models.

The Cbx5KO, T28KO (TRIM28KO) and T28HP1box (TRIM28-L2/HP1box) mouse strains were described previously [22,38,68]. Exons 2 to 4 within the *Cbx1* gene (HP1β), and exon 3 within the *Cbx3* gene (HP1γ) were surrounded by LoxP sites. Excision of the floxed exons exclusively in hepatocytes by using mice that express the Cre recombinase under the control of the albumin promoter (Alb-Cre mice, [23]) led to a frameshift within the CSD-encoding sequence of *Cbx1* and the CD-encoding sequence of *Cbx3*.

Mice were housed in a pathogen-free barrier facility, and experiments were approved by the national ethics committee for animal warfare (n°CEEA-36).

Antibodies/oligonucleotides

The anti-TRIM28 and HP1 were previously described [64, 65]. Anti-Casp3A (9661, Cell Signaling); anti-γH2AX (Ab11174, Abcam), anti-Ki67 (M3064, Spring Bioscience). Anti-5mC (NA81, Calbiochem), anti-H3K9me3 (Active Motif, 39161), anti-H3-K27me3 (Milipore, 07-449), H4K20me3 (Upstate, 07-463). Oligonucleotides are described in Supplementary Table 11.

Tissue processing for histology.

For fresh frozen tissues, 3mm sections of the liver large lobe were embedded in the OCT compound (TissueTek) following standard protocols, and 18µm-thick sections were cut using a Leica CM1850 cryostat and stored at −80 °C.

For paraffin-embedded tissues, 3mm sections of the liver large lobe were fixed in 4% neutral-buffered formalin (VWR Chemicals) at room temperature (RT) overnight, and stored in 70% ethanol at 4°C. Fixed tissues were processed using standard protocols and embedded in paraffin wax. Three-µm-thick sections were cut using a Thermo Scientific Microm HM325 microtome, dried at 37 °C overnight and stored at 4 °C.

Immunofluorescence analysis.

Cryo-sections and cultured cells were fixed in formaldehyde (2%) at RT for 15min air dried at RT for 20min and processed as described previously [38].

Immunohistochemistry.

Paraffin-embedded liver sections were processed for routine hematoxylin, eosin and Safran or reticulin staining. For immunohistochemistry, sections were processed according to standard protocols. Images were acquired with a Zeiss Apotome2 microscope and processed using ImageJ.

RNA extraction and RT-qPCR assays

RNA was isolated from liver samples using TRIzol, according to the manufacturer's recommendations (Life technologies). Reverse transcription was performed with Superscript III according to the manufacturer protocol (Invitrogen). 1/100 of this reaction was used for real-time qPCR amplification using SYBR Green I (SYBR Green SuperMix, Quanta).

RNA-seq

The details are described in supplementary methods. Data are available at GEO (accession numbers: GSE84734 and GSE119244).

ChIP

ChIP were performed according to Abcam's protocol.

Statistics and reproducibility.

The Microsoft Excel or biostatgv (*https://biostatgv.sentiweb.fr*) softwares were used for statistical analyses; statistical tests, number of independent experiments, and P-values are listed in the individual figure legends. All experiments were repeated at least twice unless otherwise stated.

ACKNOWLEDGMENTS:

We thank P. Chambon, C. Sardet, T. Forné, D.Fisher and C. Grimaud for helpful discussions and critical reading of the manuscript. We thank F. Bernex and L. LeCam, C. Keime and B. Jost for fruitful discussions. We thank L. Papon, H. Fontaine and C. Bonhomme for technical assistance and M. Oulad-Abdelghani and the IGBMC for the anti-HP1 and TRIM28 antibodies. We also thank the RHEM technical facility and particularly J. Simony for histological analysis and the IGBMC/ICS transgenic and animal facility for the initial establishment of the HP1 and TRIM28 mouse models. We thank C. Vincent and the IRCM animal core facility for the day to day care of the animal models. Finally, we thank S. Chamroeun for counting positive cells on TMA. We acknowledge the imaging facility MRI, member of the national infrastructure France-BioImaging and supported by the French National Research Agency (ANR-10-INBS-04, «Investments for the future»).

This work was supported by funds from the Centre National de la Recherche Scientifique (CNRS), the Institut National de la Santé et de la Recherche Médicale (INSERM), the University of Montpellier and the Institut regional de Cancérologie de Montpellier (ICM),) and SIRIC Montpellier Cancer, Grant INCa_Inserm_DGOS_12553. SH was funded by an Erasmus PhD fellowship. We also thank the Ministry of Education, Science and Technology of the Republic of Kosovo for a scholarships to support SH. FC was supported by grants from ANR (ANR 2009 BLAN 021 91; ANR-16CE15-0018-03), INCa (PLBIO13-146), ARC (PJA20131200357), and La ligue Régionale contre le Cancer (128-R13021FF-RAB13006FFA). Sequencing was performed by the MGX facility. Montpellier, France.

AUTHORS' CONTRIBUTIONS:

NS and SH performed the analysis of mice and interpreted the data. MP and CB made the libraries, generated and analyzed the RNA-seq data. AZ and EF performed the RT-qPCR experiments. CG participated to mice analysis, NP supervised the histological core facility and JYN performed the TMA. LK performed the pathological analysis of histological sections. DG was involved in the establishment of BMEL cells. YP and EJ were involved in cell transformation assays and chromatin analysis. FC designed, analyzed and interpreted the data and wrote the manuscript with input from all co-authors.

DECLARATION OF INTEREST: No competing interests

REFERENCES

1 Prakash K, Fournier D. Evidence for the implication of the histone code in building the genome structure. *BioSystems* 2018; **164**: 49–59.

2 Koschmann C, Nunez FJ, Mendez F, Brosnan-Cashman JA, Meeker AK, Lowenstein PR *et al.* Mutated Chromatin Regulatory Factors as Tumor Drivers in Cancer. *Cancer Res* 2017; **77**: 227–233.

3 Mirabella AC, Foster BM, Bartke T. Chromatin deregulation in disease. *Chromosoma* 2016; **125**: 75–93.

4 Mai S. The 3D Cancer Nucleus. *Genes Chromosomes Cancer* 2018. doi:10.1002/gcc.22720.

5 Janssen A, Colmenares SU, Karpen GH. Heterochromatin: Guardian of the Genome. *Annu Rev Cell Dev Biol* 2018. doi:10.1146/annurev-cellbio-100617-062653.

6 James TC, Elgin SC. Identification of a nonhistone chromosomal protein associated with heterochromatin in Drosophila melanogaster and its gene. *Mol Cell Biol* 1986; **6**: 3862–3872.

7 Eissenberg JC, Elgin SCR. HP1a: a structural chromosomal protein regulating transcription. *Trends Genet* 2014; **30**: 103–110.

8 Lomberk G, Wallrath L, Urrutia R. The Heterochromatin Protein 1 family. *Genome Biol* 2006; **7**: 228.

9 Dinant C, Luijsterburg MS. The emerging role of HP1 in the DNA damage response. *Mol Cell Biol* 2009; **29**: 6335–6340.

10 Fanti L, Pimpinelli S. HP1: a functionally multifaceted protein. *Curr Opin Genet Dev* 2008; **18**: 169–174.

11 Nishibuchi G, Nakayama J. Biochemical and structural properties of heterochromatin protein 1: understanding its role in chromatin assembly. *J Biochem* 2014; **156**: 11–20.

12 Shi S, Larson K, Guo D, Lim SJ, Dutta P, Yan S-J *et al.* Drosophila STAT is required for directly maintaining HP1 localization and heterochromatin stability. *Nat Cell Biol* 2008; **10**: 489–496.

13 Bosch-Presegué L, Raurell-Vila H, Thackray JK, González J, Casal C, Kane-Goldsmith N *et al.* Mammalian HP1 Isoforms Have Specific Roles in Heterochromatin Structure and Organization. *Cell Rep* 2017; **21**: 2048–2057.

14 Dialynas GK, Vitalini MW, Wallrath LL. Linking Heterochromatin Protein 1 (HP1) to cancer progression. *Mutat Res* 2008; **647**: 13–20.

15 Vad-Nielsen J, Nielsen AL. Beyond the histone tale: HP1α deregulation in breast cancer epigenetics. *Cancer Biology & Therapy* 2015; **16**: 189–200.

16 Janssen A, Colmenares SU, Karpen GH. Heterochromatin: Guardian of the Genome. *Annu Rev Cell Dev Biol* 2018. doi:10.1146/annurev-cellbio-100617-062653.

17 Herquel B, Ouararhni K, Khetchoumian K, Ignat M, Teletin M, Mark M *et al.* Transcription cofactors TRIM24, TRIM28, and TRIM33 associate to form regulatory complexes that suppress murine hepatocellular carcinoma. *Proc Natl Acad Sci USA* 2011; **108**: 8212–8217.

18 Fan DN-Y, Tsang FH-C, Tam AH-K, Au SL-K, Wong CC-L, Wei L *et al.* Histone lysine methyltransferase, suppressor of variegation 3-9 homolog 1, promotes hepatocellular carcinoma progression and is negatively regulated by microRNA-125b. *Hepatology* 2013; **57**: 637–647.

19 Bojkowska K, Aloisio F, Cassano M, Kapopoulou A, Santoni de Sio F, Zangger N *et al.* Liver-specific ablation of Krüppel-associated box-associated protein 1 in mice leads to male-predominant hepatosteatosis and development of liver adenoma. *Hepatology* 2012; **56**: 1279–1290.

20 Khetchoumian K, Teletin M, Tisserand J, Mark M, Herquel B, Ignat M *et al.* Loss of Trim24 (Tif1alpha) gene function confers oncogenic activity to retinoic acid receptor alpha. *Nat Genet* 2007; **39**: 1500–1506.

21 Hardy T, Mann DA. Epigenetics in liver disease: from biology to therapeutics. *Gut* 2016; **65**: 1895–1905.

22 Allan RS, Zueva E, Cammas F, Schreiber HA, Masson V, Belz GT *et al.* An epigenetic silencing pathway controlling T helper 2 cell lineage commitment. *Nature* 2012; **487**: 249–253.

23 Postic C, Shiota M, Niswender KD, Jetton TL, Chen Y, Moates JM *et al.* Dual roles for glucokinase in glucose homeostasis as determined by liver and pancreatic beta cell-specific gene knock-outs using Cre recombinase. *J Biol Chem* 1999; **274**: 305–315.

24 Weisend CM, Kundert JA, Suvorova ES, Prigge JR, Schmidt EE. Cre activity in fetal albCre mouse hepatocytes: Utility for developmental studies. *Genesis* 2009; **47**: 789–792.

25 Kuo LJ, Yang L-X. Gamma-H2AX - a novel biomarker for DNA double-strand breaks. *In Vivo* 2008; **22**: 305–309.

26 Niu Z-S, Niu X-J, Wang W-H. Genetic alterations in hepatocellular carcinoma: An update. *World J Gastroenterol* 2016; **22**: 9069–9095.

27 Bruix J, Sherman M. Management of hepatocellular carcinoma: An update. *Hepatology* 2011; **53**: 1020–1022.

28 Strick-Marchand H, Weiss MC. Inducible differentiation and morphogenesis of bipotential liver cell lines from wild-type mouse embryos. *Hepatology* 2002; **36**: 794–804.

29 Guengerich FP. Cytochrome P450 research and The Journal of Biological Chemistry. *J Biol Chem* 2018. doi:10.1074/jbc.TM118.004144.

30 Bhattacharyya S, Sinha K, Sil PC. Cytochrome P450s: mechanisms and biological implications in drug metabolism and its interaction with oxidative stress. *Curr Drug Metab* 2014; **15**: 719–742.

31 Park JW, Reed JR, Brignac-Huber LM, Backes WL. Cytochrome P450 system proteins reside in different regions of the endoplasmic reticulum. *Biochem J* 2014; **464**: 241–249.

559 32 Paik Y-H, Kim J, Aoyama T, De Minicis S, Bataller R, Brenner DA. Role of NADPH
560 oxidases in liver fibrosis. *Antioxid Redox Signal* 2014; **20**: 2854–2872.

561 33 Yang P, Wang Y, Macfarlan TS. The Role of KRAB-ZFPs in Transposable Element
562 Repression and Mammalian Evolution. *Trends Genet* 2017; **33**: 871–881.

563 34 O'Geen H, Squazzo SL, Iyengar S, Blahnik K, Rinn JL, Chang HY *et al.* Genome-wide
564 analysis of KAP1 binding suggests autoregulation of KRAB-ZNFs. *PLoS Genet* 2007; **3**:
565 e89.

566 35 Ecco G, Cassano M, Kauzlaric A, Duc J, Coluccio A, Offner S *et al.* Transposable
567 Elements and Their KRAB-ZFP Controllers Regulate Gene Expression in Adult Tissues.
568 *Dev Cell* 2016; **36**: 611–623.

569 36 Herquel B, Ouararhni K, Martianov I, Le Gras S, Ye T, Keime C *et al.* Trim24-repressed
570 VL30 retrotransposons regulate gene expression by producing noncoding RNA. *Nat*
571 *Struct Mol Biol* 2013; **20**: 339–346.

572 37 Ecco G, Imbeault M, Trono D. KRAB zinc finger proteins. *Development* 2017; **144**: 2719–
573 2729.

574 38 Herzog M, Wendling O, Guillou F, Chambon P, Mark M, Losson R *et al.* TIF1β
575 association with HP1 is essential for post-gastrulation development, but not for Sertoli
576 cell functions during spermatogenesis. *Dev Biol* 2011; **350**: 548–558.

577 39 Huang C, Su T, Xue Y, Cheng C, Lay FD, McKee RA *et al.* Cbx3 maintains lineage
578 specificity during neural differentiation. *Genes Dev* 2017; **31**: 241–246.

579 40 Mattout A, Aaronson Y, Sailaja BS, Raghu Ram EV, Harikumar A, Mallm J-P *et al.*
580 Heterochromatin Protein 1β (HP1β) has distinct functions and distinct nuclear distribution
581 in pluripotent versus differentiated cells. *Genome Biol* 2015; **16**. doi:10.1186/s13059-015-
582 0760-8.

583 41 Eissenberg JC, Morris GD, Reuter G, Hartnett T. The heterochromatin-associated protein
584 HP-1 is an essential protein in Drosophila with dosage-dependent effects on position-
585 effect variegation. *Genetics* 1992; **131**: 345–352.

586 42 Schott S, Coustham V, Simonet T, Bedet C, Palladino F. Unique and redundant functions
587 of C. elegans HP1 proteins in post-embryonic development. *Dev Biol* 2006; **298**: 176–
588 187.

589 43 Fausto N, Campbell JS, Riehle KJ. Liver regeneration. *Hepatology* 2006; **43**: S45-53.

590 44 Kurinna S, Barton MC. Cascades of transcription regulation during liver regeneration. *Int*
591 *J Biochem Cell Biol* 2011; **43**: 189–197.

592 45 Lee Y-H, Ann DK. Bi-phasic expression of Heterochromatin Protein 1 (HP1) during
593 breast cancer progression: Potential roles of HP1 and chromatin structure in
594 tumorigenesis. *J Nat Sci* 2015; **1**: e127.

595 46 Towbin BD, González-Aguilera C, Sack R, Gaidatzis D, Kalck V, Meister P *et al.* Step-
596 Wise Methylation of Histone H3K9 Positions Heterochromatin at the Nuclear Periphery.
597 *Cell* 2012; **150**: 934–947.

47 Poleshko A, Mansfield KM, Burlingame CC, Andrake MD, Shah NR, Katz RA. The human protein PRR14 tethers heterochromatin to the nuclear lamina during interphase and mitotic exit. *Cell Rep* 2013; **5**: 292–301.

48 Lehnertz B, Ueda Y, Derijck AAHA, Braunschweig U, Perez-Burgos L, Kubicek S *et al.* Suv39h-mediated histone H3 lysine 9 methylation directs DNA methylation to major satellite repeats at pericentric heterochromatin. *Curr Biol* 2003; **13**: 1192–1200.

49 Velazquez Camacho O, Galan C, Swist-Rosowska K, Ching R, Gamalinda M, Karabiber F *et al.* Major satellite repeat RNA stabilize heterochromatin retention of Suv39h enzymes by RNA-nucleosome association and RNA:DNA hybrid formation. *Elife* 2017; **6**. doi:10.7554/eLife.25293.

50 Pogribny IP, Ross SA, Tryndyak VP, Pogribna M, Poirier LA, Karpinets TV. Histone H3 lysine 9 and H4 lysine 20 trimethylation and the expression of Suv4-20h2 and Suv-39h1 histone methyltransferases in hepatocarcinogenesis induced by methyl deficiency in rats. *Carcinogenesis* 2006; **27**: 1180–1186.

51 Brustel J, Kirstein N, Izard F, Grimaud C, Prorok P, Cayrou C *et al.* Histone H4K20 tri-methylation at late-firing origins ensures timely heterochromatin replication. *EMBO J* 2017; **36**: 2726–2741.

52 Jørgensen S, Schotta G, Sørensen CS. Histone H4 lysine 20 methylation: key player in epigenetic regulation of genomic integrity. *Nucleic Acids Res* 2013; **41**: 2797–2806.

53 Du Q, Bert SA, Armstrong NJ, Caldon CE, Song JZ, Nair SS *et al.* Replication timing and epigenome remodelling are associated with the nature of chromosomal rearrangements in cancer. *Nat Commun* 2019; **10**: 416.

54 Lee DH, Li Y, Shin D-H, Yi SA, Bang S-Y, Park EK *et al.* DNA microarray profiling of genes differentially regulated by three heterochromatin protein 1 (HP1) homologs in Drosophila. *Biochem Biophys Res Commun* 2013; **434**: 820–828.

55 Piacentini L, Fanti L, Negri R, Del Vescovo V, Fatica A, Altieri F *et al.* Heterochromatin protein 1 (HP1a) positively regulates euchromatic gene expression through RNA transcript association and interaction with hnRNPs in Drosophila. *PLoS Genet* 2009; **5**: e1000670.

56 Vakoc CR, Mandat SA, Olenchock BA, Blobel GA. Histone H3 lysine 9 methylation and HP1gamma are associated with transcription elongation through mammalian chromatin. *Mol Cell* 2005; **19**: 381–391.

57 Stunnenberg R, Kulasegaran-Shylini R, Keller C, Kirschmann MA, Gelman L, Bühler M. H3K9 methylation extends across natural boundaries of heterochromatin in the absence of an HP1 protein. *EMBO J* 2015; **34**: 2789–2803.

58 Takaki A, Yamamoto K. Control of oxidative stress in hepatocellular carcinoma: Helpful or harmful? *World J Hepatol* 2015; **7**: 968–979.

59 Cizkova K, Konieczna A, Erdosova B, Lichnovska R, Ehrmann J. Peroxisome Proliferator-Activated Receptors in Regulation of Cytochromes P450: New Way to Overcome Multidrug Resistance? *J Biomed Biotechnol* 2012; **2012**. doi:10.1155/2012/656428.

60 Del Campo JA, Gallego P, Grande L. Role of inflammatory response in liver diseases: Therapeutic strategies. *World J Hepatol* 2018; **10**: 1–7.

641 61 Bishayee A. The role of inflammation and liver cancer. *Adv Exp Med Biol* 2014; **816**:
642 401–435.

643 62 Pogribny IP, Rusyn I. Role of epigenetic aberrations in the development and progression
644 of human hepatocellular carcinoma. *Cancer Lett* 2014; **342**: 223–230.

645 63 Brégnard C, Guerra J, Déjardin S, Passalacqua F, Benkirane M, Laguette N.
646 Upregulated LINE-1 Activity in the Fanconi Anemia Cancer Susceptibility Syndrome
647 Leads to Spontaneous Pro-inflammatory Cytokine Production. *EBioMedicine* 2016; **8**:
648 184–194.

649 64 Matsui T, Leung D, Miyashita H, Maksakova IA, Miyachi H, Kimura H *et al.* Proviral
650 silencing in embryonic stem cells requires the histone methyltransferase ESET. *Nature*
651 2010; **464**: 927–931.

652 65 Kato M, Takemoto K, Shinkai Y. A somatic role for the histone methyltransferase Setdb1
653 in endogenous retrovirus silencing. *Nat Commun* 2018; **9**: 1683.

654 66 Jacobs FMJ, Greenberg D, Nguyen N, Haeussler M, Ewing AD, Katzman S *et al.* An
655 evolutionary arms race between KRAB zinc-finger genes ZNF91/93 and SVA/L1
656 retrotransposons. *Nature* 2014; **516**: 242–245.

657 67 Wolf G, Yang P, Füchtbauer AC, Füchtbauer E-M, Silva AM, Park C *et al.* The KRAB
658 zinc finger protein ZFP809 is required to initiate epigenetic silencing of endogenous
659 retroviruses. *Genes Dev* 2015; **29**: 538–554.

660 68 Cammas F, Mark M, Dollé P, Dierich A, Chambon P, Losson R. Mice lacking the
661 transcriptional corepressor TIF1beta are defective in early postimplantation development.
662 *Development* 2000; **127**: 2955–2963.

663

664

LEGENDS FIGURES

Figure 1: **HP1 proteins are essential to prevent tumour development in liver**. (A) Schematic representation of the strategy to inactivate the two HP1-encoding genes (*Cbx1*, *3*) specifically in hepatocytes using the recombinase Cre expressed under the control of the albumin promoter in WT or HP1αKO mice. (B) Western blot analysis of whole-cell extracts from liver samples confirmed the absence of HP1α (the residual band is due to the very high level of immunoglobulins in liver and thus the presence of light chains that are of the same size as HP1α) and the decreased expression of HP1β and HP1γ due to the hepatocytes-specific excision of the corresponding genes in HP1-TKO as compared to age-matched control mice. Ponceau staining was used as loading control. (C) Graph showing the percentage of animals developing tumors (morphological and histological analysis). Controls (Ctl; n=109; 6.4%), HP1αKO (HP1a KO; n= 73; 8.5%), HP1β-liverKO (HP1b KO; n=17; 52.9%), HP1γ-liverKO (HP1g KO; n=37; 13.5%), HP1α/HP1β-liverKO (HP1ab KO; n=8; 50%), HP1α/HP1γ-liverKO (HP1ag; KO n=12; 25%) and HP1α/HP1β/HP1γ-liverKO (HP1-TKO, n=19; 78.9%). The exact Fisher statistical test was used for each genotype versus control, **p value ≤0.01; ***p value ≤0.001 (D) Examples of morphology of livers with tumors (arrows) in animals for each HP1 knockout combination. The liver morphology of a female and a male age-matched controls are also shown (F Ctl and M Ctl, respectively). (E) Histological analysis (hematoxylin-eosin-Safran staining) of one representative HP1-TKO female (F-TKO) and one representative HP1-TKO male (M-TKO) livers. Upper panels: tumor/liver parenchyma interface highlighted by arrowheads (low magnifications). Bottom panels: magnification (x 100) of the boxes in the upper panels showing the tumor in the right part of the images (thick plates of atypical hepatocytes). A venous tumor thrombus is also present (asterisk).(F) RT-qPCR analysis of the expression of the indicated genes in control (Ctl, n=5) and HP1-TKO (TKON: normal liver, n=6; TKOT: tumor, n=5) livers of animals older that one year. RT-qPCR data were normalized to *Hprt* expression and are shown as the mean ± SEM. *p value <0.05; ***p value <0.001, ns: not significant (Student's t-test).

Figure 2 : HP1-TKO hepatic cells are viable and have increased potential to cellular transformation upon oncogenic stress. (A) Schematic representation of the strategy used to establish BMEL cells from *Cbx5*-/-; *Cbx1*L2/L2; *Cbx3*L2/L2 fetal livers and to inactivate the three HP1-encoding genes. Western blot analysis of whole-cell extracts from Het, Ctl and HP1-TKO BMEL cells. "Het" were *Cbx5*+/-; *Cbx1*L2/L2 BMEL cells, "HP1-TKO" and "Ctl" were established clones originating from one *Cbx5*-/-; *Cbx1*L2/L2; *Cbx3*L2/L2; Cre-ERT clone treated (KO1 and KO3) or not (C3 and C5) with tamoxifen respectively. HP1-TKO cells were stably transfected with a plasmid (pCX, chicken β-actin promoter) allowing the expression of YFP either alone (RCtl) or in fusion with HP1β (RHP1b) (B) Proliferation curves of 2 Control clones (C3 and C5) and 2 HP1-TKO clones (KO1 and KO3). The graph represent the average of three independent experiments done in triplicates. Student t-test analysis showed no significant difference between control and HP1-TKO clones (C) HP1-TKO cells have a higher capacity of forming clones from isolated cells than control cells. Representative pictures of clonogenic assays performed on the two control (C3 and C5) and HP1-TKO (KO1 and KO3) clones with the graph representing the average of 5 independent experiments. (D) HP1-TKO cells are more resistant than control cells to the expression of the oncogene Ras-V12. Representative images of control (C3 and C5) and HP1-TKO (KO1 and KO3) BMEL cells transduced with either an empty (control) or a Ras-V12 (Ras-V12) expressing lentivirus and grown for 8 days after the transduction. (E) HP1-TKO cells are more prone to transformation than control cells in response to Ras-V12 and SV40 oncogenes expression. Representative images of control (C3 and C5) and HP1-TKO (KO1 and KO3) BMEL cells transduced with either an empty (control) or two Ras-V12 (Ras-V12) and SV40 expressing lentivirus respectively (Ras-V12+SV40) grown for 8 days after the transduction on culture dishes and then grown for 20 days in soft agar. Graph represented the average of three independent experiments. Results are shown as the mean number of colonies ± SEM. *p value <0.05; (Student's t-test).

Figure 3: **HP1 are essential for the maintenance of heterochromatin marks but not to regulate the expression of major satellites**. (A) Western blot analysis of nuclear extracts from livers of 7-week-old and middle-aged (3-6-month-old) controls (Ctl: 1; 2; 5; 6) and HP1-TKO (TKO: 3; 4; 7; 8) mice with antibodies against the indicated histone marks. Ponceau staining was used as loading control. (B) Western blot analysis of whole cell extracts of one Het (lane 1), two (lanes 2-3) controls, two (lanes 4-5) HP1-TKO and two (lanes 6-7) HP1-TKO clones expressing HP1β-YFP (RHP1b) fusion protein with the indicated antibodies. (C) IF analysis of H3K9me3, H3K27me3, 5mC and LamB1 in BMEL cells. (D) Loss of HP1 leads to a partial relocation of DAPI-dense regions towards the nuclear periphery. Representative images of paraffin-embedded liver tissue sections from 7-week-old control (Ctl) and HP1-TKO (TKO) mice stained with DAPI (63x magnification). To select mostly hepatocytes, only the largest nuclei with a size comprised between 70 and 150 μm^2 and with a circular shape were selected for this analysis. 2D sections of nuclei were divided in four concentric areas (1 to 4) and DAPI staining intensity was quantified using the cell profiler software. The mean fractional intensity at a given radius was calculated as the fraction of the total intensity normalized to the fraction of pixels at a given radius in n=584 control and n=762 HP1-TKO (TKO) nuclei. Data are the mean ± SEM. ***p value <0.001. (E) ChIP analysis of H3K9me3 and H3K27me3 enrichment on major satellite repeats within control (Ctl, C3 and C5) and HP1-TKO (TKO, KO1 and KO3) BMEL cells. Graphs represent the average of 5 independent experiments and are shown as the mean ± SEM. ***p value <0.001, ns: not significant (Student's t-test). (F) Loss of the three HP1 proteins did not affect the expression of major satellites in neither liver nor BMEL cells. qPCR assays were performed using total RNA from livers of 7-week-old control (n=4) and HP1-TKO mice (n=4) and on control (Ctl, C3 and C5) and HP1-TKO (TKO, KO1 and KO3) BMEL cells. data were normalized to *Hprt* expression and are shown as the mean ± SEM. ns: not significant (Student's t-test). (G) Satellite repeats were quantified by qPCR on genomic DNA from the same animals as those used for (F).

Figure 4: **HP1 are essential regulators of gene expression in liver.** (A) MA plot after DSeq2 normalization of RNA-seq data from 7-week-old control (n=3) and HP1-TKO (n=4) liver RNA samples. Red dots represent genes that are differentially expressed between control and HP1-TKO mice (adjusted p-value p <0.05). (B) Functional clustering of HP1-dependent genes using the DAVID Gene Ontology software. (C) RT-qPCR analysis of the expression of the indicated genes. RNA was extracted from livers of 7-week old control (Ctl) and HP1-TKO (TKO) mice. (D) RT-qPCR analysis of the expression of 4 *krabzfp* genes (*zfp951*, *zfp992*, *zfp984* and *5730507C01Rik* (573Rik)) whose expression was found to be deregulated in both HP1αβ-liverKO and HP1-TKO livers by RNA-seq analysis and 1 *krabzfp* gene (*zfp345*) deregulated in both HP1αγ-liverKO and HP1-TKO livers by RNA-seq analysis. cDNA were prepared from livers of 5-weeks old controls (Ctl), HP1αβ-liverKO (HP1αβKO) and HP1αγ-liverKO (HP1αγKO). RT-qPCR data were normalized to *Hprt* expression and are shown as the mean ± SEM. Statistical analysis were made between expression in controls and expression in the different HP1-mutant samples. *p value <0.05; ***p value <0.001, ns: not significant (Student's t-test).

Figure 5: **HP1 are required for silencing specific endogenous retroviruses (ERVs) in hepatocytes.** (A) MA-plot after DSeq2 normalization of RNA-seq reads including repeats aligned against the Repbase database. Red dots represent genes and repeats that are differentially expressed between controls and HP1-TKO liver samples (p<0.05). (B) Distribution of the different families of retrotransposons amongst repeats that are up-regulated upon loss of HP1 (Repeat_Up) compared to repeats that are down-regulated (Repeat_Down) and to the genome-wide distribution of repeats according to the RepeatMasker database (All). (C) Repeats over-expressed in HP1-TKO liver samples compared with controls (Repeat_Up) are over-represented in regions (± 100kb) around genes over-expressed in HP1-TKO (genes_up). Conversely, repeats down-regulated in HP1-TKO liver samples compared with controls (Repeat_Down) are over-represented in regions (± 100kb) around genes repressed in HP1-TKO (genes_down). (D) Repeats that are up-

772 regulated or down-regulated upon HP1 loss tend to be closer to genes that are up- or down-
773 regulated in HP1-TKO, respectively. The absolute distance (in base pairs) was measured
774 between the gene transcriptional start site and the beginning of the repeat, according to the
775 RepeatMasker annotation. (E) Representative Integrative Genomic Viewer snapshots of the
776 indicated up-regulated genes associated with up-regulated repeat sequences. (F) RT-qPCR
777 analysis of the expression of the indicated genes in Control (Ctl) and HP1-TKO (TKO) BMEL
778 cells. (G) RT-qPCR analysis of the expression of the indicated genes in Control rescue (RCtl)
779 and HP1β rescue (RHP1b) BMEL cell lines. RT-qPCR data were normalized to *Hprt* and
780 *36B4* expression and are shown as the mean ± SEM. **p* value <0.05; ****p* value <0.001, ns:
781 not significant (Student's t-test). (H) ChIP analysis of H3K9me3 enrichment in the 3'UTR
782 regions of *zfp345*, *zfp951* and *zfp992*, in the P2, IAP and p4 regions of the *Bglap3* gene
783 locus [35]. **p* value <0.05; ***p* value <0.01, ****p* value <0.001, ns: not significant (Student's t-
784 test).

785 **Figure 6**: **The loss of association between HP1 and TRIM28 partially recapitulates the**
786 **phenotypes induced by the loss of HP1.** (A) TRIM28 expression is independent of HP1
787 proteins. RT-qPCR quantification of TRIM28 expression in total RNA from livers of 7-week-
788 old control (Ctl; n=4) and HP1-TKO (TKO; n=4) mice. Data were normalized to *Hprt*
789 expression and are shown as the mean ± SEM. (B) Western blot analysis of 50µg of whole
790 cell extracts from 7-week-old control (1 and 2) and HP1-TKO (3 to 5) livers using an anti-
791 TRIM28 polyclonal antibody. Tubulin was used as loading control. (C) The loss of interaction
792 between TRIM28 and HP1 does not significantly alter the level of expression of neither
793 TRIM28 or HP1. 50 µg of whole liver extracts from 7-week-old controls (1; 2), TRIM28KO
794 (T28KO; 3-5) and TRIM29HP1box (T28HP1box; 6-8) mice were analyzed by western blotting
795 using the anti-TRIM28 polyclonal and anti-HP1α, β and γ monoclonal antibodies. GAPDH
796 and Ponceau staining were used as loading controls. (D) TRIM28 is involved in the
797 regulation of the expression of some but not all HP1-dependent genes. RT-qPCR analysis
798 using liver RNA samples from 5 week-old control (n=5), T28KO (n=5) and T28HP1box (n=5)

mice. (E) TRIM28 is involved in the regulated expression of HP1- and ERV-dependent genes. Analysis of *Mbd1* and *Bglap3* expression by RT-qPCR using liver RNA samples from 7-week-old control (Ctl) and HP1-TKO (TKO) mice, and 5-week-old control (n=5), T28KO (n=5) and T28HP1box (n=5) mice. (F) TRIM28 and its association with HP1 is essential to prevent liver tumor development. Representative morphological aspect of TRIM28 mutant livers. (G) *Bglap3* and *Mbd1* are over-expressed in HP1-TKO livers of old (>1year) mice. RT-qPCR was performed using RNA from old control (n=7), and HP1-TKO liver samples (TKON for normal part, TKOT for tumor part) (n=7). (H) The alteration of *Mbd1* and *Bglap3* expression upon loss of the association between TRIM28 and HP1 proteins was not maintained in old animals. RT-qPCR analysis using RNA from control (n=5), T28KO (T28KON for normal part, T28KOT for tumor part) (n=5) and T28HP1box (T28HP1boxN for normal part, T28HP1boxT for tumor part) livers (n=5). All expression data were normalized to *Hprt* expression and are shown as the mean ± SEM. ns, no significant difference **p* value <0.05; ***p* value <0.01; ****p* value <0.001 (Student's t-test).

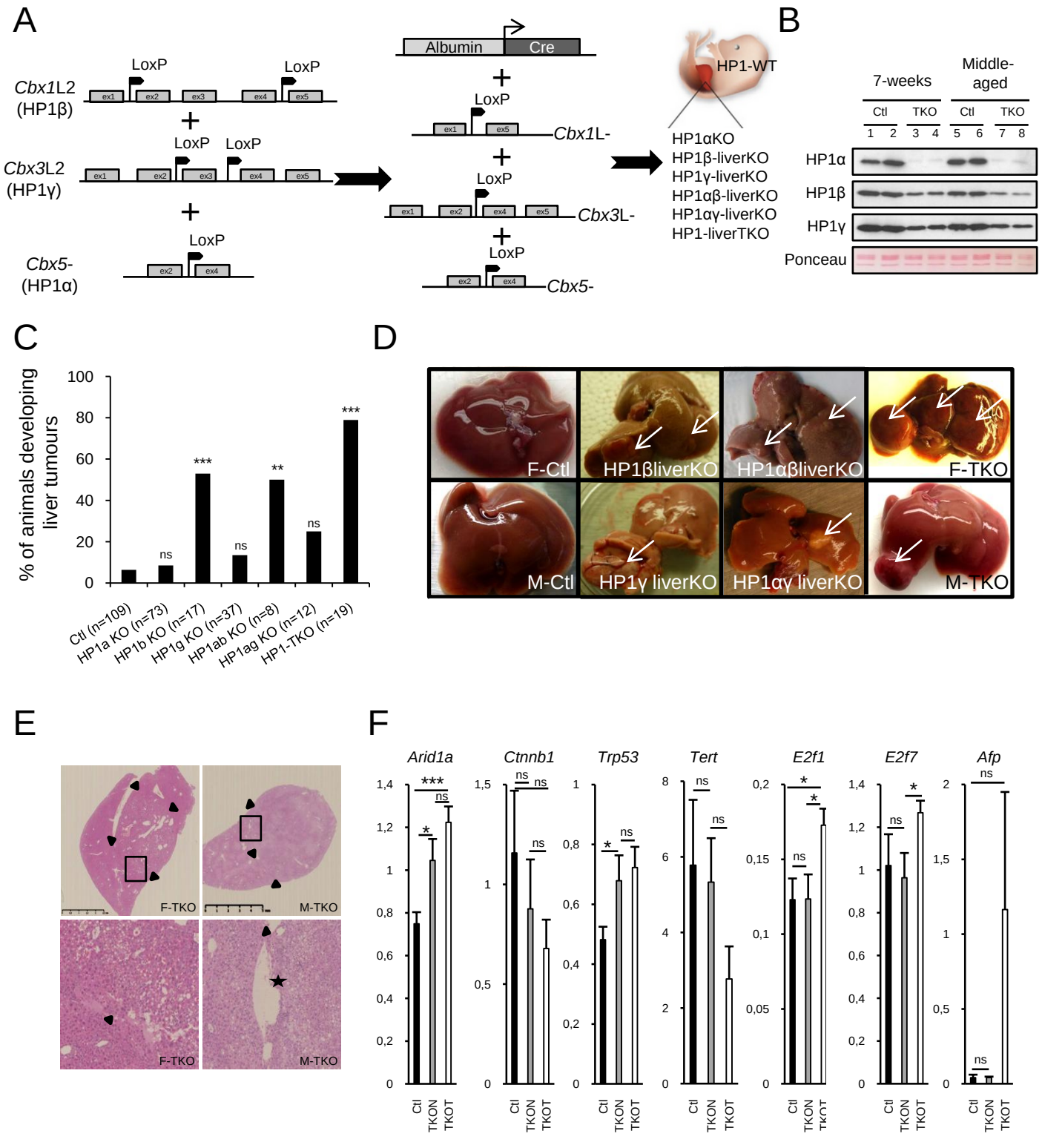

Figure 1, Saksouk & Hajdari et al,

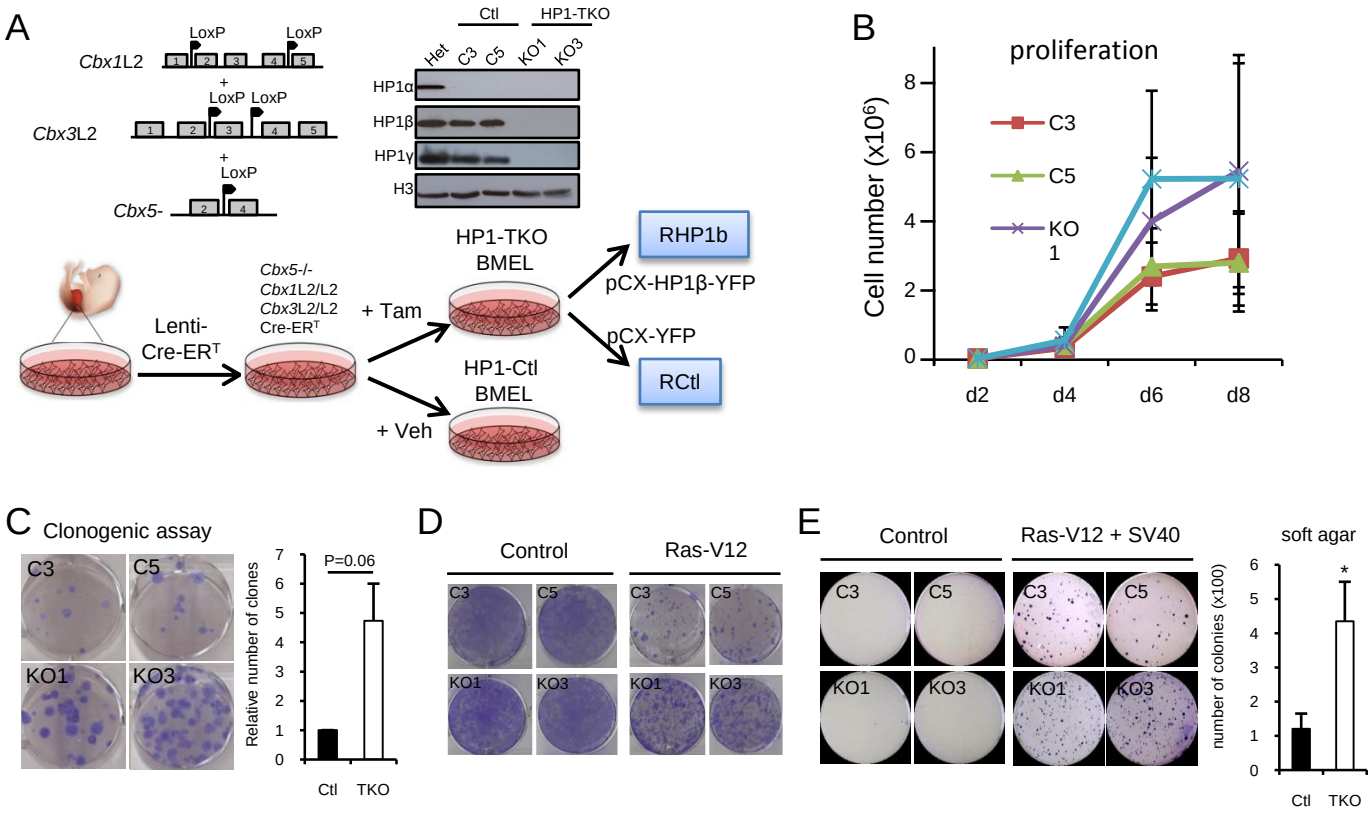

Figure 2. Saksouk & Hajdari et al.

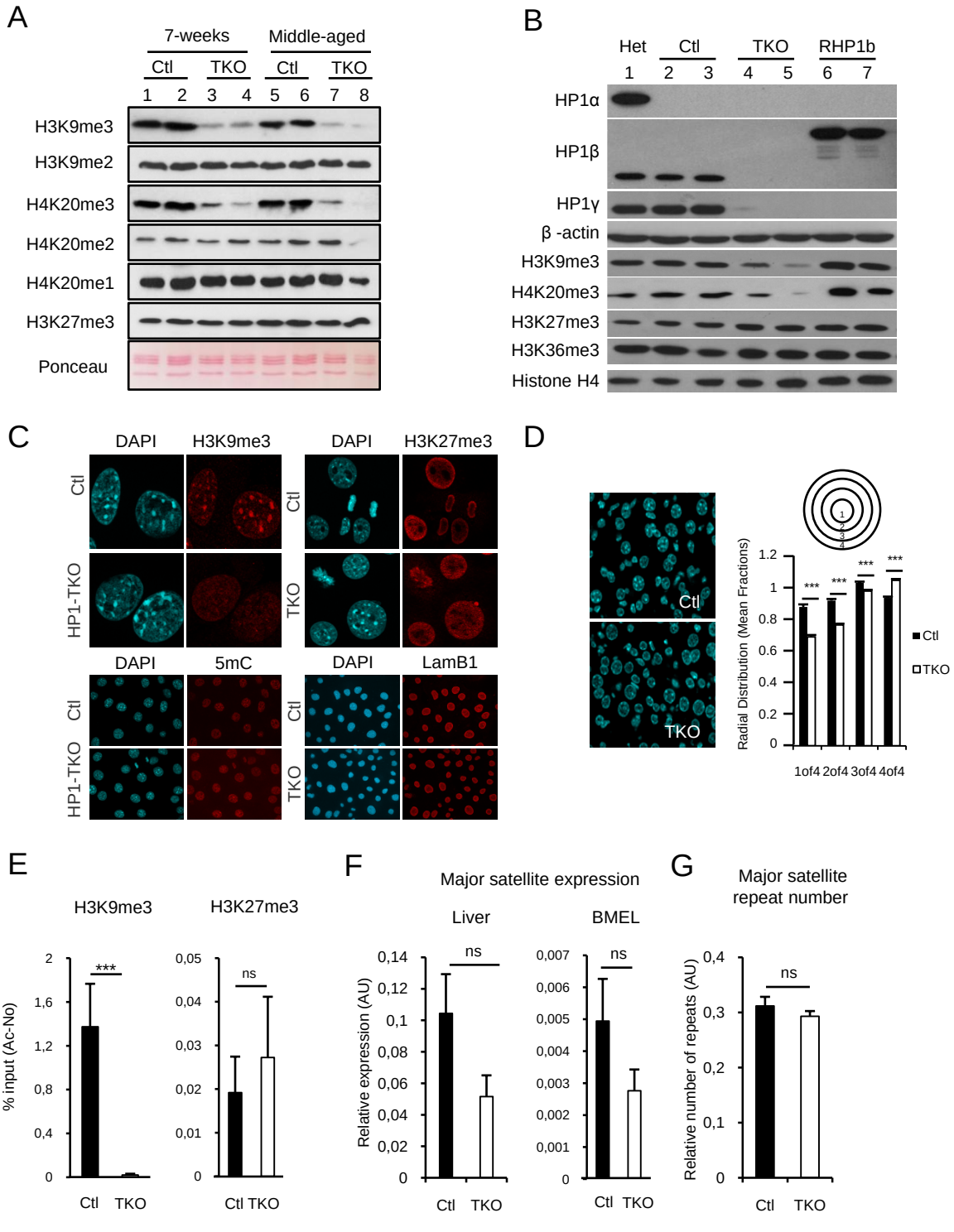

Figure 3, Saksouk, Hajdari et al,

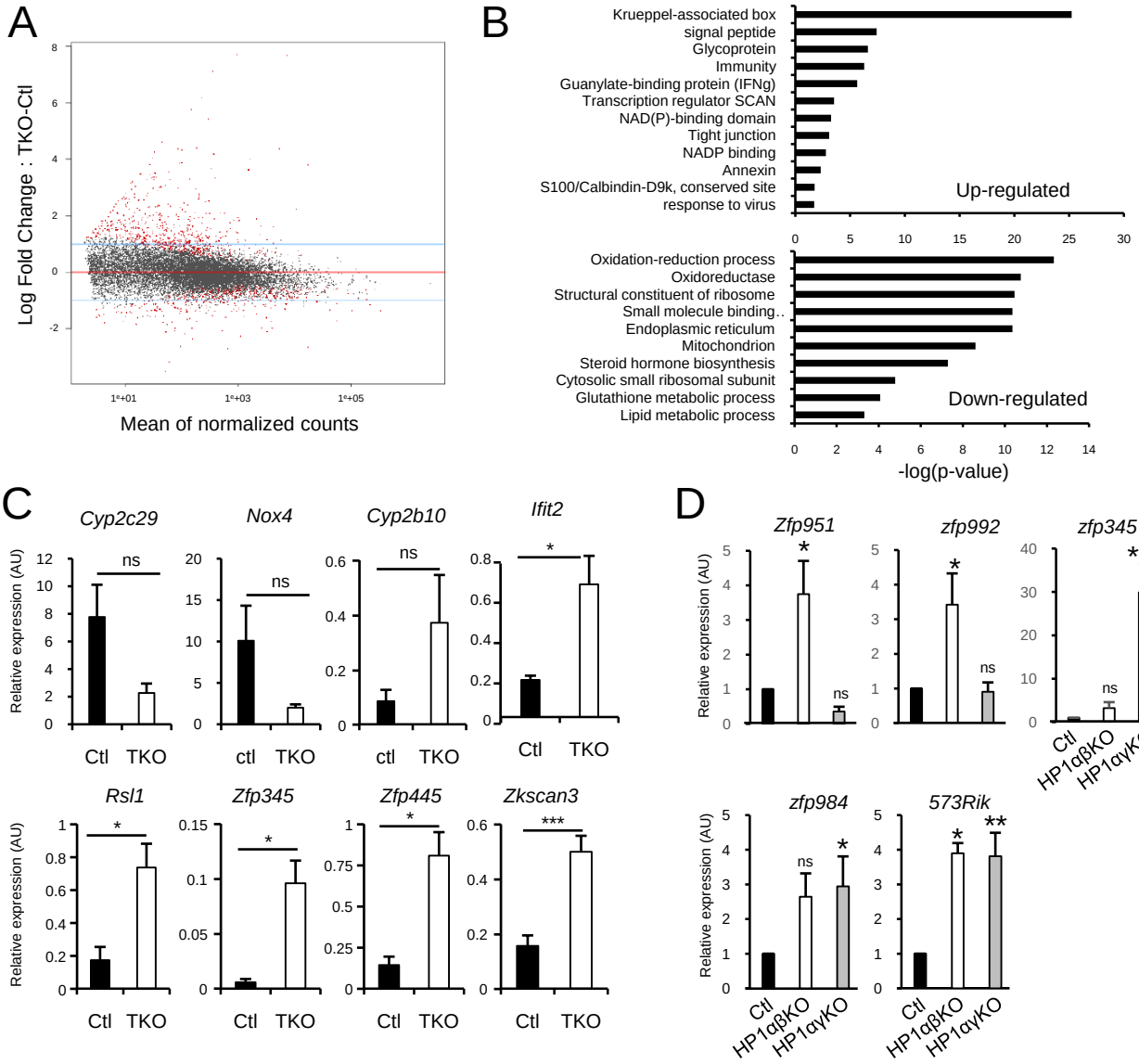

Figure 4 Saksouk & Hajdari et al,

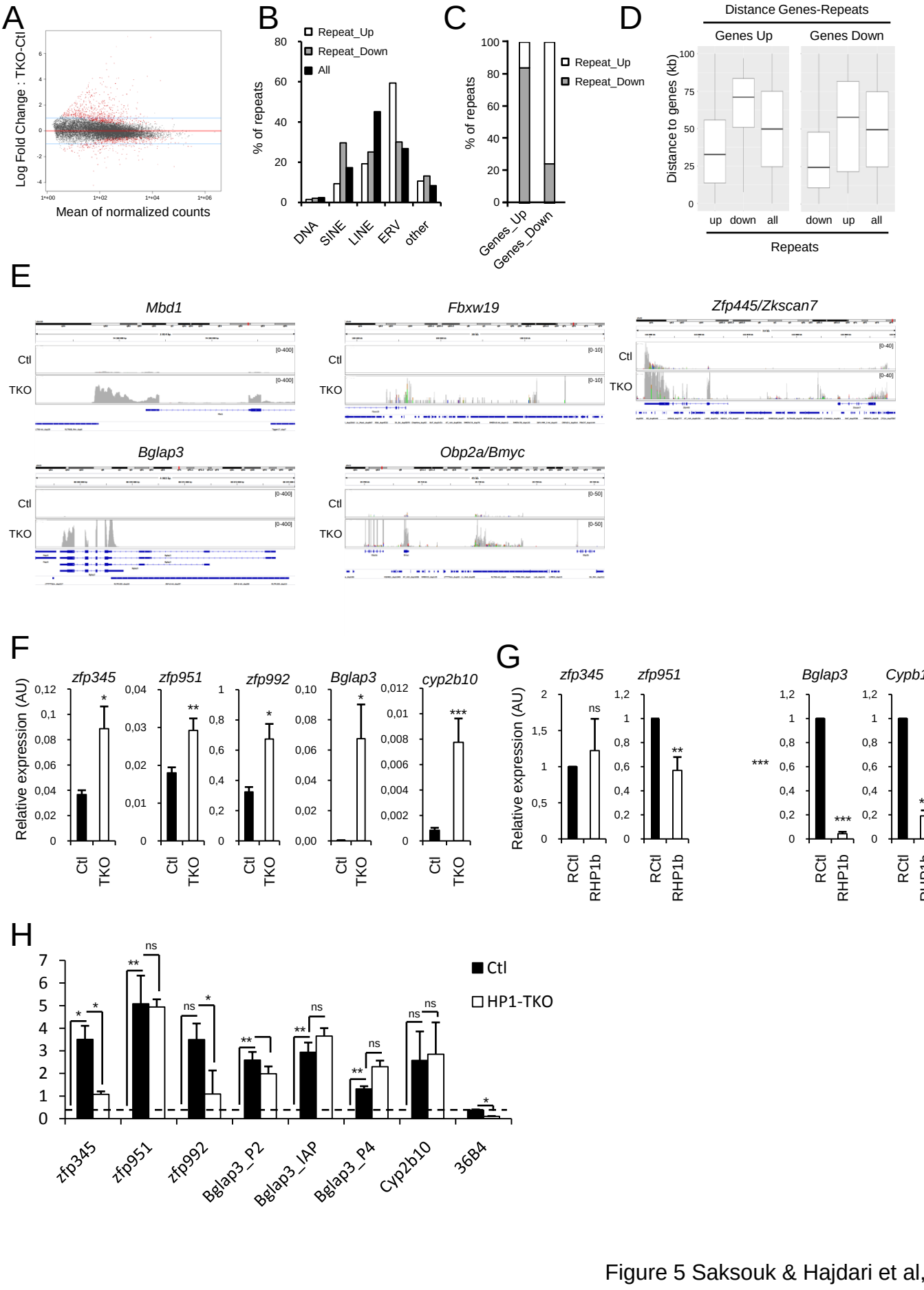

Figure 5 Saksouk & Hajdari et al,

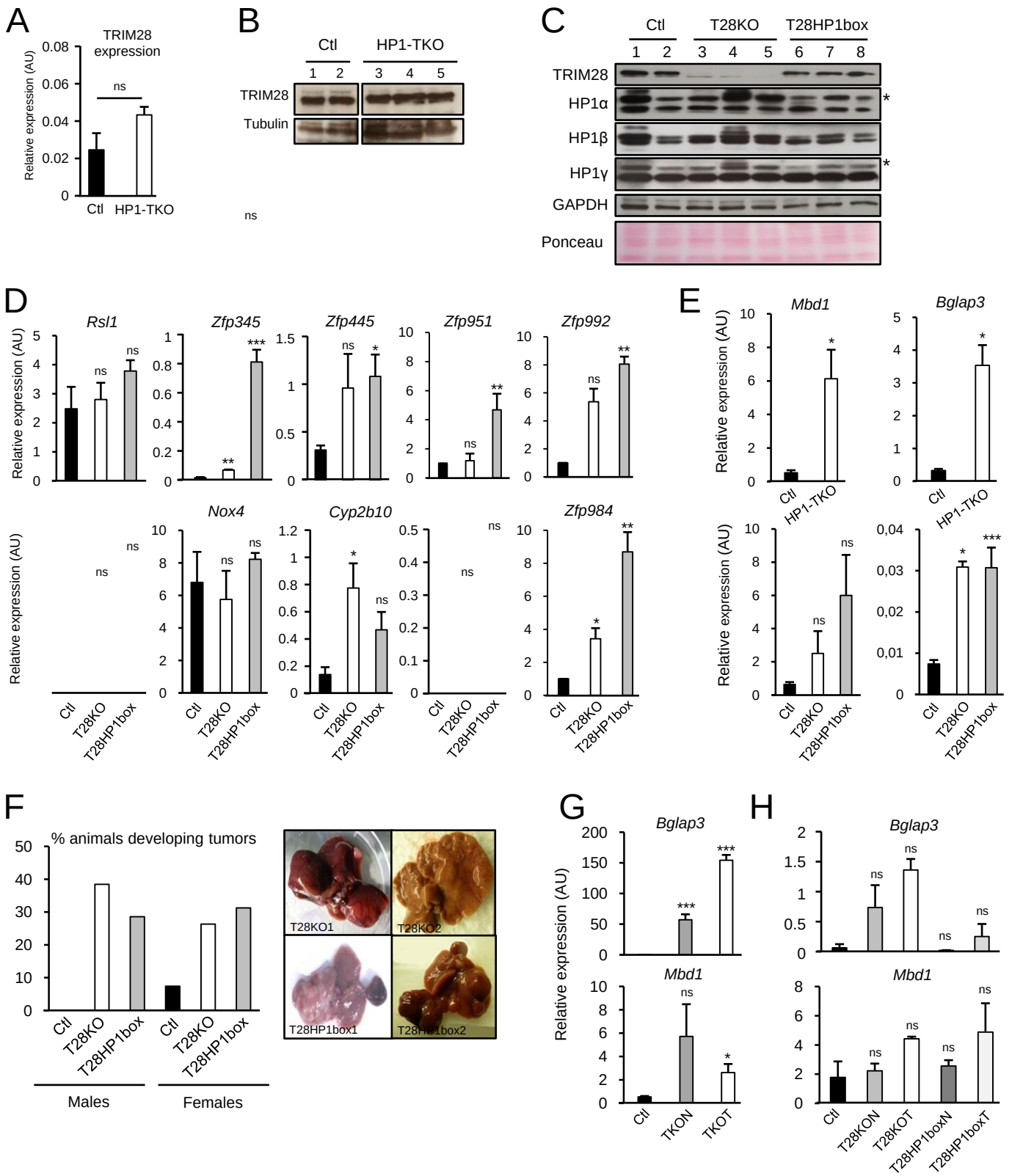

Figure 6, Saksouk & Hajdari et al,

Table 1: HP1-dependent p450 genes.

Gene name	Log2 fold-change	padj	Redox	Endoplasmic reticulum	Drug metabolism	Lipid metabolism	Steroid synthesis
Cyp2b10	4.06	1.41E-38	1	1	0	0	1
Cyp2b9	2.68	4.51E-10	1	1	0	0	1
Cyp2b13	1.80	0.000120	0	0	0	0	1
Cyp4f16	1.63	1.36E-09	0	0	0	0	0
Cyp2d12	1.38	0.000468	0	0	0	0	1
Cyp2a4	1.09	0.0342	0	0	0	0	0
Cyp2a22	1.06	0.000559	0	0	0	0	0
Cyp2f2	-0.65	0.00318	1	1	0	0	0
Cyp4f13	-0.67	0.0151	0	0	0	0	0
Cyp2r1	-0.72	0.0173	1	1	0	0	0
Cyp27a1	-0.83	1.30E-05	1	0	0	0	0
Cyp2d37-ps	-0.83	0.0319	0	0	0	0	0
Cyp3a25	-0.85	0.00222	1	1	0	0	1
Cyp39a1	-0.88	0.00164	1	1	0	1	0
Cyp2e1	-0.94	7.81E-05	1	1	1	0	1
Cyp2d26	-0.95	2.57E-05	1	1	0	0	1
Cyp2a5	-0.97	0.00129	0	0	0	0	0
Cyp2d13	-1.00	0.00445	0	0	0	0	0
Cyp1a2	-1.25	3.65E-12	1	1	1	1	1
Cyp2c53-ps	-1.31	0.01178	0	0	0	0	0
Cyp2d40	-1.42	6.83E-06	0	0	0	0	1
Cyp46a1	-1.64	0.000629	1	1	0	1	0
Cyp3a59	-2.15	3.62E-17	1	0	0	0	0
Cyp2c44	-2.20	2.18E-20	0	0	0	0	1
Cyp2c29	-2.60	7.65E-25	1	1	0	0	1

(1) found and (0) not found according to the David Gene Ontology software.